

Revealing the substrate origin of the linear dispersion of silicene/Ag(111)

M. X. Chen and M. Weinert

Department of Physics, University of Wisconsin, Milwaukee, Wisconsin 53211, USA

(Dated: August 15, 2014)

The band structure of the recently synthesized (3×3) silicene monolayer on (4×4) Ag(111) is investigated using density functional theory. A k -projection technique that includes the k_{\perp} -dependence of the surface bands is used to separate the contributions arising from the silicene and the substrate, allowing a consistent comparison between the calculations and the angle-resolved photoemission experiments. Our calculations not only reproduce the observed gap and linear dispersion across the K point of (1×1) silicene, but also demonstrate that these originate from the k_{\perp} -dependence of Ag(111) substrate states (modified by interactions with the silicene) and *not* from a Dirac state.

PACS numbers: 71.20.-b, 73.20.-r, 73.22.Pr

The recent theoretical prediction of silicene, the silicon counterpart of graphene, has generated intense interest in this new two-dimensional system [1]. Unlike graphene, silicene is predicted to have a low-buckled honeycomb structure, in which one Si atom is buckled out of the plane, but the linear band dispersion at the K point – the Dirac states – is preserved by the crystal symmetry. While graphene can be mechanically exfoliated from graphite, silicene has to be grown on a substrate.[2–4] Recently, silicene monolayers were epitaxially grown on Ag(111) [3–10] and various structures were reported by scanning tunneling microscopy (STM) experiment, such as (3×3) [5] and $(\sqrt{3}\times\sqrt{3})$ [6] reconstructions with respect to ideal silicene. The existence of Dirac states in silicene/Ag(111), however, remains hotly debated. Angle-resolved photoemission spectroscopy (ARPES) experiments for (3×3) silicene on (4×4) Ag(111) show a linear dispersion and a gap forming around the K point of (1×1) silicene [5]. Linear dispersion above the Fermi level (E_F) was also deduced from STM experiments [6, 9] for the $(\sqrt{3}\times\sqrt{3})$ reconstruction of silicene/Ag(111). In contrast, the Landau levels for (3×3) -silicene on (4×4) Ag(111) [henceforth referred to as silicene/Ag(111)] in a magnetic field are distinct from those of graphite, suggesting the absence of a Dirac point in the system [11].

There have been a number of density functional theory (DFT) calculations to clarify whether the Dirac point exists in silicene/Ag(111) and explain the nature of the linear band observed by ARPES experiment [12–18]. The linear dispersion was not seen in these DFT calculations. Instead, Refs. 14 and 15 show that a Ag band has similar dispersion to the linear band observed by ARPES, and Ref. 16 claims that the linear dispersion results from the hybridization between silicene and the substrate since such a state disappears in the pure substrate. Further ARPES experiments[18–20] observe similar spectral features, but have attributed the linear dispersion to gapped silicene bands[19], hybridized metallic surface states[20], or silicene-induced Ag free-electron states.[18] Despite the considerable research devoted to this system, attempts to establish a link between the DFT calculations

and the experimental observations are at present incomplete since the calculations have not been able to provide a consistent explanation of the experimental results for both the clean substrate and the silicene/Ag(111) system.

In this paper, we use a k -projection unfolding scheme [21, 22] to reconcile the experimental observations and the calculations for both the pure Ag(111) substrate and silicene/Ag(111). We demonstrate that the linear dispersion is not due to Dirac states of the silicene, but rather due to substrate states that are modified by the interaction with the silicene. The experimental observations are demonstrated to be consistent with the k_{\perp} -dependence of the bands probed by the photoemission experiments.

In our calculations, the Ag(111) surface substrate is modeled by a ten-atomic-layer slab, which is separated from its periodic images by ~ 20 Å vacuum regions. Silicene monolayers are symmetrically placed on both sides of the substrate slab to avoid dipole interactions between slabs. The electronic and structural properties are calculated using the local density approximation and VASP [23, 24] with the projector augmented wave potentials to represent the ion cores. The surface Brillouin zone (BZ) is sampled by k -point meshes that are equivalent to the 6×6 Γ -centered Monkhorst-Pack mesh for a (4×4) cell. Atoms in the middle eight layers of the Ag substrate are frozen at the bulk geometry, while all other atoms are fully relaxed until the residual forces are less than 0.001 eV/Å. The influence of van der Waals (vdW) dispersion forces between the adsorbate and the substrate were examined using dispersion-corrected DFT-D3 calculations[25]: the additional forces (and subsequent changes in atomic positions) were found to be within the force convergence criteria, reflecting the relative importance of the direct Si-Ag bonding.

The unfolded bands are obtained using the k -projection method [21, 22] in which the projection of a function ψ that transforms as the irreducible representation of the translation group labeled by \mathbf{k} is given by

$$\psi_{\mathbf{k}} = \hat{P}_{\mathbf{k}} \psi = \frac{1}{h} \sum_{\mathbf{t}} \chi_{\mathbf{k}}^*(\mathbf{t}) \hat{T}_{\mathbf{t}} \psi,$$

where $\hat{T}_{\mathbf{t}}$ is the translational operator corresponding to the translation \mathbf{t} with character $\chi_{\mathbf{k}}(\mathbf{t}) = e^{i\mathbf{k}\cdot\mathbf{t}}$, and where the set $\{\mathbf{t}\}$ of order h corresponds to the translations associated with a cell defined by direct and reciprocal lattice vectors \mathbf{a}_i and \mathbf{b}_j , respectively. In practice, ψ is most often a wave function calculated at \mathbf{k}_s of a supercell (defined by lattice vectors \mathbf{A}_i and \mathbf{B}_j), and $\psi_{\mathbf{k}}$ is the projection on to the primitive cell. (The projection may be on to an even smaller cell: for example, in the case of Cu_3Au [21] the unit cell is simple cubic, but an fcc “primitive” cell is appropriate for describing the Cu bands.)

For plane-wave-based representations of the wave functions with commensurate primitive and super-cells, this procedure is particularly simple, reducing to the problem of determining which \mathbf{k}_p each plane wave $e^{i\mathbf{G}\cdot\mathbf{r}}$ belongs to, i.e., for integers M_i and m_j , determining the fractional part κ_j that defines \mathbf{k}_p of the primitive cell relative to \mathbf{k}_s of the supercell:

$$\begin{aligned}\mathbf{G} &= \sum_i M_i \mathbf{B}_i = \sum_j (m_j + \kappa_j) \mathbf{b}_j \\ &= \sum_j \left(\sum_i M_i (\mathbf{B}_i \cdot \mathbf{a}_j) \right) \mathbf{b}_j,\end{aligned}$$

with $\mathbf{a}_i \cdot \mathbf{b}_j = \delta_{ij}$. For an ideal supercell, this decomposition is exact since it is a simple consequence of translational symmetry and recovers the primitive band structure with $\langle \psi_{\mathbf{k}_p} | \psi_{\mathbf{k}_p} \rangle = 1$ or 0, while for defect systems, the norm will be between zero and one. Once a wave function has been k -projected, its weight $|\psi_{\mathbf{k}}(\mathbf{r})|^2$ in different spatial regions (or over all space) can be obtained by straightforward integration, which is particularly useful for interface structures. As shown below for silicene/Ag(111), a layer projection along z separates the k -projected band structure for the silicene overlayer and the Ag substrate.

Our relaxed silicene/Ag(111) structure, Fig 1(a), is distorted compared to ideal free-standing silicene: six atoms that reside above Ag atoms are shifted up, resulting in a new structure that has a mirror symmetry about the (110) plane. Moreover, the buckling ($\sim 0.9\text{\AA}$) is significantly enhanced in silicene/Ag(111), almost twice that of the ideal silicene, implying strong perturbations of the silicene bands due to interactions with the substrate. The simulated STM image for this structure is in good agreement with experiments and previous DFT simulations [5, 11–13, 16]. Because of this reconstruction, the degeneracy and linear dispersion at K_{Si} seen for the ideal (1×1) silicene, Fig. 1(b) is no longer required by symmetry.

Although the distorted silicene no longer has the (1×1) silicene periodicity, the bands can still be unfolded into the silicene BZ by projecting the supercell wave functions onto the corresponding k of the (1×1) silicene cell. Figures 1(c,d) depict the k -projected band structure of the distorted silicene without the substrate, where the

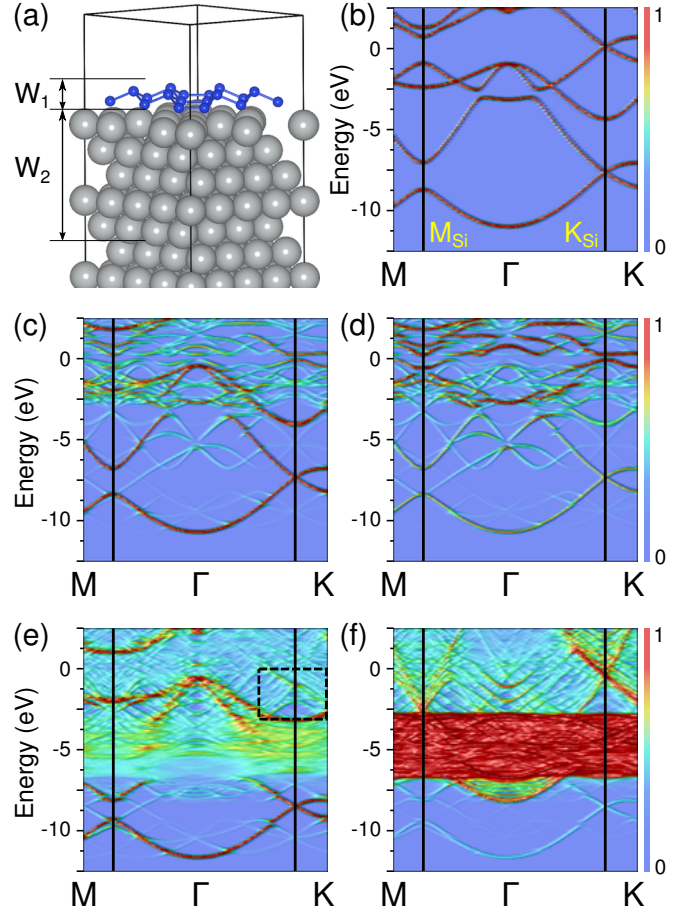


FIG. 1. (a) Perspective view of the relaxed structure of (3×3) silicene on (4×4) Ag(111). W_1 (centered on the silicene) and W_2 (substrate) are the spatial regions used for integrating wave functions in k -projection. k -projected bands for (b) ideal free-standing silicene; for free-standing distorted silicene, weighted by the contributions (c) in the silicene layer (W_1) and (d) in the vacuum region above the layer; and for silicene/Ag(111), weighted by the wave function contributions in (e) W_1 and (f) W_2 . K and M (K_{Si} and M_{Si}) correspond to the high symmetry points of the (1×1) Ag (silicene) surface Brillouin zone, and $E_F = 0$. The black dashed box in (e) indicates the experimental window probed by ARPES [5]. The color bars indicate the layer- and k -projected weights of the bands relative (between 0 and 1) to the maximum in the plot; the same color scheme is used in subsequent figures also.

k -projected bands are weighted by a layer-integration over the wave functions in the silicene layer (Fig. 1(c)) and the vacuum region (Fig. 1(d)) to facilitate investigation of silicene-substrate interaction to be discussed later. While the σ bands of the ideal silicene are fairly well preserved in the distorted structure, the linear π and π^* bands around the K_{Si} are strongly perturbed, leading to a gap opening at the Fermi level because of the symmetry breaking associated with the (3×3) structural reconstruction, consistent with previous calculations [26]. Because the silicene π orbitals extend farther into the

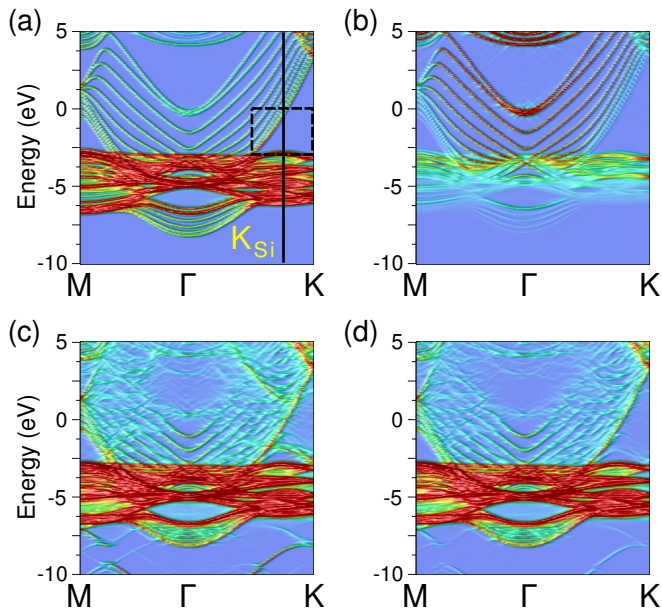


FIG. 2. Bands k -projected to the (1×1) Ag(111) for: the Ag(111) surface in (a) the substrate (W_2) and (b) vacuum (W_1); and for silicene/Ag(111) in (c) both the silicene and the substrate, $W_1 + W_2$, and (d) the substrate only, W_2 . The dashed black box in (a) indicates the experimental window of ARPES [5]. Solid black lines mark the K_{Si} point, and $E_F = 0$.

vacuum than the σ ones, they will have more overlap, and hence interaction, with the Ag substrate states.

For the interacting (distorted) silicene-Ag(111) system, the bands k -projected onto (1×1) silicene, Fig. 1(e), show that the σ bands of silicene are similar, although shifted down in energy by $\sim 1-2$ eV. The π states, however, are strongly modified, with the result that the (gapped) π states in the isolated (distorted) silicene around K_{Si} are indistinct in the E vs. k window corresponding to the ARPES experiments indicated by the black box.

The bands projected on to (1×1) silicene but weighted by their contribution in the substrate, Fig. 1(f), are dominated by the Ag d bands around -5 eV and the free-electron sp bands. (Because the projection is to the silicene cell, rather than (1×1) Ag, the d states do not project to specific k values, but rather almost uniformly in k . Projecting to the Ag cell as in Fig. 2 recovers the momentum resolution; the sp states, being free-electron-like, are not sensitive to the k -projection used.) The two nearly linear Ag-derived bands intersecting at K_{Si} near the Fermi level reflect the folding of the bands due to the (3×3) periodicity associated with the silicene overlayer, not a symmetry-dictated Dirac cone. Similar unfoldings were done in Refs. 14 and 16 for silicene/Ag(111), but the remaining band foldings hid the substrate nature of bands.

Figure 2 shows k -projected bands of Ag(111) without and with silicene, for the k -projection done with respect to (1×1) Ag(111). Since now the projection is to the

“correct” reference, the dispersion of the Ag d bands is well-defined. Comparison of Figs. 2(a) and (c) shows essentially no changes in the Ag d bands when the silicene is adsorbed. Because of the finite number of layers in the Ag substrate, the sp bulk band is represented by a set of 10 bands in Fig. 2 which have spectral weight within the E vs. k window probed experimentally [5], and thus should be accessible to ARPES measurement. In particular, the band edge state crosses K_{Si} with almost linear dispersion. By comparing the spatial distributions of the states in Figs. 2(a,b), the higher energy sp states have greater surface weight, suggesting that these states will have the greatest overlap with the silicene.

For the silicene/Ag(111) case, Figs. 2(c,d), a comparison of the dispersion and intensity of bands with those of the Ag(111) surface indicates that the observed linear band is predominately derived from substrate. Comparing Fig 2(d) with Fig 1(d), the crossing at the K_{Si} point disappears when the bands are completely unfolded, confirming the absence of the Dirac cone in silicene/Ag(111).

We now discuss the relation between our DFT calculations and the experimental observations. Because the wave functions of silicene/Ag(111) are dominated by silicene in W_1 and by the substrate in W_2 , respectively, a reasonable approximation to the experiment observation is to use the k -projected bands appropriate to the underlying translational symmetry of the different spatial regions, i.e., for silicene, W_1 [Fig 1(e)], and for the substrate, W_2 [Fig 2(d)]. The calculations thus show that the linear band in Fig 2(d) due to the substrate — and not a silicene band — should be identified with the one observed by ARPES.

A consistent interpretation to the experimental observations requires explanations for the origin of the linear band across the K_{Si} ; for the parabolic bands near the M and Γ points; for the gap opening at the K_{Si} , M, and Γ points for silicene/Ag(111); and the absence of bands in the experimental range for the pure substrate [5, 19]. Previously, Ref. 16 attributed the linear band observed by ARPES to a new hybridized state due to the strong silicene-substrate interaction because it disappears in pure Ag(111), while our calculations suggest that it is a (modified) substrate state, either a surface resonance near the bottom of the sp band or a true surface state split off from the bottom of the band. (Because of the finite number of layers used to represent the substrate, determining whether this lowest band is at or just below the band edge is difficult to determine; the increased localization in the surface region compared to the clean substrate is consistent with either case.) Moreover, whether a state is observed or not in ARPES is not simply a matter of whether or not it is hybridized. Refs. 14 and 15 show that the linear band observed by ARPES looks similar to one of Ag bands in the projected effective band structure, but the relationship between the experiments and calculations was not explored.

Our results for the pure substrate indicate that there are some Ag bands in the experimental range [Fig. 2(a)] which were, however, not observed by APRES. Because these bands are bulk bands, they have a strong k_{\perp} -dependence due to the large band widths (cf., Fig. 2(a)). By choosing particular photon energies, the ARPES experiments [5] could choose a window with no bulk Ag states visible. To make quantitative connection with the experiments, we thus need to account for the experimental conditions.

We address these issues by including in the k -projection the momentum perpendicular to the surface, k_{\perp} , probed by the photoelectron, i.e.,

$$k_{\perp} = \sqrt{\frac{2m_e}{\hbar^2} (h\nu - \phi - |E_B|) - \mathbf{k}_{\parallel}^2}, \quad (1)$$

where $h\nu$ is the photon energy, ϕ is the work function of the system, E_B is the binding energy of electrons, and \mathbf{k}_{\parallel} is the component parallel to the surface of the electron crystal momentum (with both k_{\perp} and \mathbf{k}_{\parallel} determined up to a reciprocal lattice vector). Our calculated work functions for the pure substrate and silicene/Ag(111) are 4.78 and 4.67 eV, respectively. The range of $|E_B|$ for the ARPES experiments in Ref. 5 is 3 eV and 1.5 eV for those in Ref. 19. For $\mathbf{k}_{\parallel} = \mathbf{K}_{\text{Si}}$ and a photon energy of 126 eV as in the experiments, k_{\perp} is in the range of 0.7–1.1 \AA^{-1} for the pure substrate, while for silicene/Ag(111) they are 2.03–2.27 \AA^{-1} along Γ -K and 0.37–0.7 \AA^{-1} for Γ -M- Γ (taking reciprocal lattice vectors into account for the estimates).

Figure 3(a) shows $E(k_{\perp})$ for the Ag(111) surface in the first BZ corresponding to fcc Ag at $\mathbf{k}_{\parallel} = \mathbf{K}_{\text{Si}}$ [27]. Not surprisingly, these are essentially the bulk bands for this \mathbf{k}_{\parallel} , with the effect of the surface showing up in the apparent increased widths of some bands and the faint weights corresponding to the energies of the band extrema. The band of particular interest is the uppermost one that starts out below E_F for small k_{\perp} and then disperses above for larger k_{\perp} . Thus this band will be seen in ARPES only for photons corresponding to small k_{\perp} . The k -projected surface bands for $k_{\perp} = 1 \text{ \AA}^{-1}$, a value corresponding roughly to the experiment, are shown in Fig. 3(b). In agreement with the experiment [5], there are no Ag states seen in the selected energy-momentum window.

Similarly, calculated $E(k_{\parallel})$ around \mathbf{K}_{Si} for silicene/Ag(111) for different values of k_{\perp} are shown in Figs. 3(c,d). For $k_{\perp} = 2.56 \text{ \AA}^{-1}$ outside the estimated experimental range of k_{\perp} , there is a band crossing \mathbf{K}_{Si} that remains continuous throughout the whole k_{\parallel} window [Fig. 3(c)]. For $k_{\perp} = 2.26 \text{ \AA}^{-1}$, which is in the estimated range of the experiment, the band shifts up in energy, and is more diffuse but also more nearly linear. Moreover, a gap of about 0.3 eV is opened just below E_F at \mathbf{K}_{Si} , in surprisingly good agreement with the ARPES experiment [5]. The k_{\perp} -dependence is also

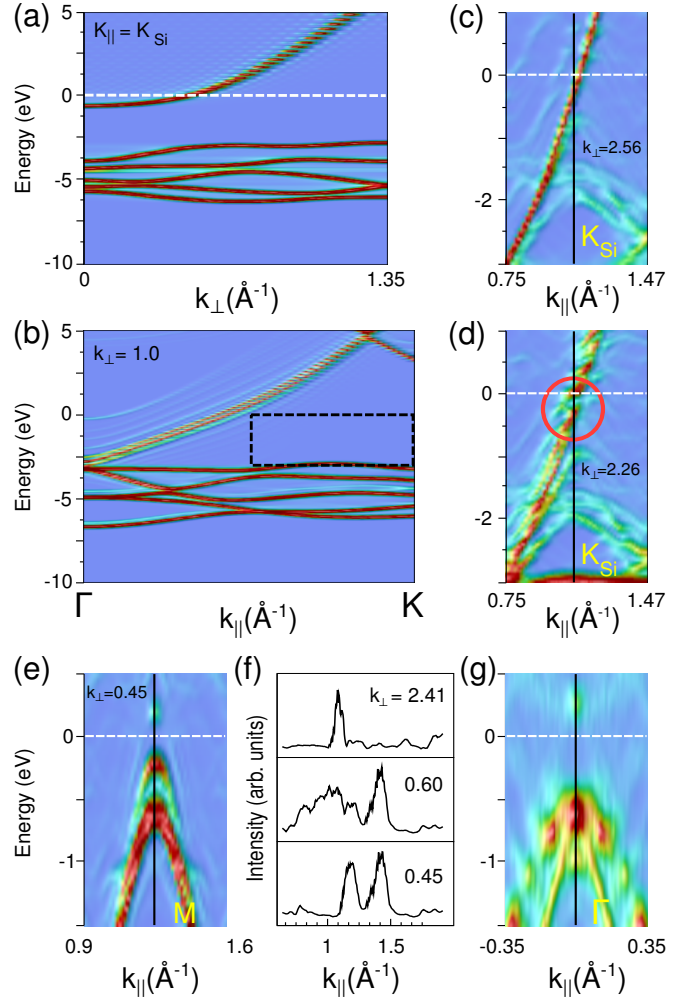


FIG. 3. (a) $E(k_{\perp})$ for $k_{\parallel} = \mathbf{K}_{\text{Si}}$ and (b) $E(k_{\parallel})$ along Γ -K with $k_{\perp} = 1.0 \text{ \AA}^{-1}$ for a 40-layer Ag(111) film. The black dashed box is the experimental window [5]. (c) $E(k_{\parallel})$ around \mathbf{K}_{Si} for silicene/Ag(111) along Γ -K for $k_{\perp} = 2.56 \text{ \AA}^{-1}$ and (d) 2.26 \AA^{-1} . (e) $E(k_{\parallel})$ around \mathbf{M} (along the Γ -M- Γ direction) for silicene/Ag(111) with $k_{\perp} = 0.45 \text{ \AA}^{-1}$. (f) Simulated momentum distribution curves along the Γ -M direction for $E_B = 1.0 \text{ eV}$ and for $k_{\perp} = 2.41, 0.60, 0.45 \text{ \AA}^{-1}$, corresponding approximately to 85, 105, and 126 eV photon energies, respectively. (g) k -projected bands around Γ for silicene in silicene/Ag(111) along K- Γ -K, weighted by contributions on Si atoms only. The k -projections for (a)–(f) were done with respect to the bulk Ag unit cell, $E_F = 0$.

consistent with more recent ARPES experiments [18, 20] (c.f., Fig. 3 in Ref. 20, and the lack of an observed gap at \mathbf{K}_{Si} for the photon energies used in Ref. 18), both for the clean Ag substrate and for the silicene/Ag system. This k_{\perp} -dependent gap opening has its origin in the changed boundary conditions that the Ag sp states see due to, for example, the presence of (and hybridization with) the silicene layer and changes in the work function, that will cause modifications to these wave functions in the near surface region. Moreover, the Fermi velocity de-

rived from the calculated band structure is $\sim 1.3 \times 10^6$ ms^{-1} , in good agreement with the experimental value[5], further indicating the substrate origin of the observed linear dispersion.

Good agreement between our calculations and experiment[18, 19] is also obtained for the bands about the M point, Fig. 3(e): the band is parabolic and separated from the Fermi level by a gap, comparable to the experimental value. (The band splitting at M in our calculation is due to the limited number (10) of Ag layers in the structural model.) Simulations of momentum distribution curves (MDC) along Γ -M- Γ were carried out for the k -projected bands of silicene/Ag(111). Our results for the MDCs around M, Fig. 3(f), show the same trend with k_{\perp} (photon energy) as the ARPES experiments in Ref. 19; that the correspondence is not perfect between the experimental photon energies [19] and our estimated values of k_{\perp} , is due in part to differences in work functions.

Bands near Γ are complicated by the remaining band folding of the Ag-derived bands noted in Fig. 1(f). To eliminate these Ag contributions, the k -projected bands are weighted by the partial density of states on the silicon atoms only. Bands along K- Γ -K are shown in Fig. 3(g), which shows two silicene bands at about -0.5 eV at Γ , with the substrate bands (cf., Fig. 2(c)) are further below starting at about -1 eV. In the experiments, however, only one silicene band with asymmetric intensity with respect to k was seen [Fig. 4(b) of Ref. 19], which we tentatively attribute to polarization and matrix elements effects similar to those demonstrated for Cu(111) [28]. While a more complete simulation of ARPES is beyond the scope of the present work, our results nevertheless indicate that all the bands about Γ in the energy window of the ARPES experiment are parabolic [Figs. 2(c) and 3(g)] and are not related to Dirac states at K_{Si} folded back to Γ .

In summary, based on first-principles calculations of the k -projected bands we have elucidated the origin of the linear dispersion observed by ARPES for silicene/Ag(111) and the observation that bands of the pure substrate are absent in the experimental window. The linear band in silicene/Ag(111) is found to originate primarily from the substrate and not from Dirac states in the silicene. To reconcile the experimental observations and the calculations for both Ag(111) and silicene/Ag(111), it is essential that the calculations account for the k_{\perp} (photon) dependence of the states. Our theoretical results provide a consistent explanation of the available experimental data, and thus resolve the controversy concerning the (non-)existence of Dirac states in silicene/Ag(111).

This work was supported by the U.S. Department of Energy, Office of Basic Energy Sciences, Division of Materials and Engineering under Award DE-FG02-07ER46228.

-
- [1] S. Cahangirov, M. Topsakal, E. Akturk, H. Sahin, and S. Ciraci, *Phys. Rev. Lett.* **102**, 236804 (2009)
 - [2] A. Fleurence, R. Friedlein, T. Ozaki, H. Kawai, Y. Wang, and Y. Yamada-Takamura, *Phys. Rev. Lett.* **108**, 245501 (2012)
 - [3] B. Lalmi, H. Oughaddou, H. Enriquez, A. Kara, S. Vizzini, B. Ealet, and B. Aufray, *Appl. Phys. Lett.* **97**, 2231092 (2010)
 - [4] H. Jamgotchian, Y. Colignon, N. Hamzaoui, B. Ealet, J. Y. Hoarau, B. Aufray, and J. P. Bibrian, *J. Phys.: Condens. Matter* **24**, 172001 (2012)
 - [5] P. Vogt, P. De Padova, C. Quaresima, J. Avila, E. Frantzeskakis, M. C. Asensio, A. Resta, B. Ealet, and G. Le Lay, *Phys. Rev. Lett.* **108**, 155501 (2012)
 - [6] L. Chen, C.-C. Liu, B. Feng, X. He, P. Cheng, Z. Ding, S. Meng, Y. Yao, and K. Wu, *Phys. Rev. Lett.* **109**, 056804 (2012)
 - [7] B. Feng, Z. Ding, S. Meng, Y. Yao, X. He, P. Cheng, L. Chen, and K. Wu, *Nano Lett.* **12**, 3507 (2012)
 - [8] A. Fleurence, R. Friedlein, T. Ozaki, H. Kawai, Y. Wang, and Y. Yamada-Takamura, *Phys. Rev. Lett.* **108**, 245501 (2012)
 - [9] L. Chen, H. Li, B. Feng, Z. Ding, J. Qiu, P. Cheng, K. Wu, and S. Meng, *Phys. Rev. Lett.* **110**, 085504 (2013)
 - [10] L. Meng, Y. Wang, L. Zhang, S. Du, R. Wu, L. Li, Y. Zhang, G. Li, H. Zhou, W. A. Hofer, and H.-J. Gao, *Nano Lett.* **13**, 685 (2013)
 - [11] C.-L. Lin, R. Arafune, K. Kawahara, M. Kanno, N. Tsukahara, E. Minamitani, Y. Kim, M. Kawai, and N. Takagi, *Phys. Rev. Lett.* **110**, 076801 (2013)
 - [12] Z.-X. Guo, S. Furuya, J.-i. Iwata, and A. Oshiyama, *J. Phys. Soc. Jpn.* **82**, 063714 (2013)
 - [13] Z.-X. Guo, S. Furuya, J.-i. Iwata, and A. Oshiyama, *Phys. Rev. B* **87**, 235435 (2013)
 - [14] Y.-P. Wang and H.-P. Cheng, *Phys. Rev. B* **87**, 245430 (2013)
 - [15] P. Gori, O. Pulci, F. Ronci, S. Colonna, and F. Bechstedt, *J. Appl. Phys.* **114**, 113710 (2013)
 - [16] S. Cahangirov, M. Audiffred, P. Tang, A. Iacomino, W. Duan, G. Merino, and A. Rubio, *Phys. Rev. B* **88**, 035432 (2013)
 - [17] R. Quhe, Y. Yuan, J. Zheng, Y. Wang, Z. Ni, J. Shi, D. Yu, J. Yang, and J. Lu, arXiv:1405.6186 [cond-mat, physics:physics](2014), arXiv: 1405.6186
 - [18] S. K. Mahatha, P. Moras, V. Bellini, P. M. Sheverdyeva, C. Struzzi, L. Petaccia, and C. Carbone, *Phys. Rev. B* **89**, 201416 (2014)
 - [19] J. Avila, P. D. Padova, S. Cho, I. Colambo, S. Lorcy, C. Quaresima, P. Vogt, A. Resta, G. L. Lay, and M. C. Asensio, *J. Phys.: Condens. Matter* **25**, 262001 (2013)
 - [20] D. Tsoutsou, E. Xenogiannopoulou, E. Golias, P. Tspas, and A. Dimoulas, *Appl. Phys. Lett.* **103**, 231604 (2013)
 - [21] J. W. Davenport, R. E. Watson, and M. Weinert, *Phys. Rev. B* **37**, 9985 (1988)
 - [22] Y. Qi, S. H. Rhim, G. F. Sun, M. Weinert, and L. Li, *Phys. Rev. Lett.* **105**, 085502 (2010)
 - [23] G. Kresse and J. Furthmüller, *Comput. Mater. Sci.* **6**, 15 (1996)
 - [24] G. Kresse and J. Furthmüller, *Phys. Rev. B* **54**, 11169 (1996)
 - [25] S. Grimme, J. Antony, S. Ehrlich, and H. Krieg, *J. Chem.*

- Phys. **132**, 154104 (2010)
- [26] P. Pflugradt, L. Matthes, and F. Bechstedt, Phys. Rev. B **89**, 035403 (2014)
- [27] For the (1×1) Ag(111) calculations, a 40-layer slab, 20 Å vacuum regions, and an 18×18 Monkhorst-Pack mesh were used.
- [28] M. Mulazzi, G. Rossi, J. Braun, J. Minar, H. Ebert, G. Panaccione, I. Vobornik, and J. Fujii, Phys. Rev. B **79**, 165421 (2009)